Analyst

Accepted Manuscript

This article can be cited before page numbers have been issued, to do this please use: X. Zhong, M. Jiang, Y. Lei, Y. Chai, Y. Zhuo and R. Yuan, *Analyst*, 2020, DOI: 10.1039/D0AN00997K.

ROYAL SOCIETY OF CHEMISTRY

rsc.li/analyst

Strong Electrochemiluminescence of Tetrakis(4-aminophenyl) ethane Doped Perylene Microcrystals for Biosensing Applications

View Article Online
DOI: 10.1039/D0AN00997K

Xia Zhong, Ming-Hui Jiang, Yan-Mei Lei, Ya-Qin Chai, Ruo Yuan, and Ying Zhuo*

School of Chemistry and Chemical Engineering, Southwest University, Chongqing 400715, PR China

*Corresponding author. E-mail: yingzhuo@swu.edu.cn (Y. Zhuo)

Abstract

Perylene and its derivatives, as classical organic polycyclic aromatic hydrocarbons (PAHs) ECL materials, have attracted extensive attention due to their excellent photoelectric activity and good structural controllability. As is well known, the molecular structure of perylene is composed of five coplanar aromatic rings. There are intense π-π stacking interactions between perylene molecules, which leads to its existence in the form of aggregates and poor solubility in aqueous media. Unfortunately, such aggregation could weaken or even quench their emission intensity owing to the aggregation-caused quenching (ACQ) effect, finally limiting the analytical application of organic luminophores in biological detection. In this work, the perylene composite microcrystals (ETTA@Pe MCs) doped with non-planar molecular tetrakis(4-aminophenyl)ethene were synthesized in aqueous phase by the surfactant assisted self-assembly method. During the process, the intense π-π stacking interactions of perylene monomers were suppressed by doping. As a result, the ETTA@Pe MCs exhibited a significantly enhanced ECL signal compared to that of alone perylene microcrystals (Pe MCs) in the case of $S_2O_8^{2-}$ as a co-reactant. Moreover, the ETTA@Pe MCs, as a novel electrochemiluminescence (ECL) luminophore, was utilized to fabricate a sensitive ECL biosensor for the quantitative analysis of dopamine (DA), which displayed favorable linear response from 1 nmol/L~100 μmol/L with detection limit of 0.96 nmol/L.

Keywords: perylene; aggregation-caused quenching; electrochemiluminescence; tetrakis(4-aminophenyl)ethane.

1. Introduction

The polycyclic aromatic hydrocarbons (PAHs) are highly attractive organic luminophores in the fields of biological sensing and optoelectronic devices [1], owning to their merits of inexpensive production, stable physical and chemical properties, structural tailorability, and high luminous efficiency [2, 3]. Usually, the PAHs can exhibit significant optical property when they are dispersed in a highly diluted solution, but become weakly luminescent or even loss of the emission in a concentrated solution

or solid films due to the aggregation-caused quenching (ACQ) effect [4-6]. Considering that many practical applications of luminophores required emission in their condensed phases (aggregates or solid films), it is inevitable to suffer the ACQ to weaken or even quench the emission. Therefore, the main challenge to improve the luminous performance of organic luminophores is the difficulty in breaking through the ACQ effect in the aggregate state.

Perylene and its derivatives, as classical polycyclic aromatic hydrocarbon electrochemiluminescence (ECL) materials, were composed of five coplanar aromatic rings to from a largely planar conjugated structure, which will lead to the strong π-π stacking between single molecules in the aggregated state and then weaken ECL emission [7]. In recent years, numerous attempts have been made to weaken or even eliminate the ACQ [8-11]. For instance, (1) to adjust the intermolecular arrangement through the formation of J-aggregates [12], (2) to manipulate the aggregate structures by the both generation of amorphous and crystalline domains [13], (3) to tune the energies of triplet and singlet exciton [14]. Although these methods can improve ECL performance to a certain extent, the control of molecular arrangement is difficult and the result is of limited effectiveness. Inspired by the concept of aggregation-induced emission (AIE) proposed in 2001 [15], Zhao and co-workers [16,17] modified the building blocks with AIE characteristics at the bay area of perylene diimide (PDI) core for changing typical ACQ molecules into AIE molecules. Subsequently, Zong et al [18] also reported that the introduction of rotatable aromatic rings as isolation groups on the sides of PDI derivatives could successfully achieve the conversion from ACQ luminophore to AIE. Interestingly, the emission enhancement of luminophore in the aggregated state becomes more pronounced as the enlarged volume of isolation groups. Despite the remarkable progress of the proposed method, the synthesis, separation and purification of modified molecules is complex and difficult. In the work, a facile and economic self-assembly method was developed by doping the non-planar tetrakis(4-aminophenyl) ethene (ETTA) into perylene solution with the assist of surfactant to obtain the novel microcrystals (ETTA@Pe MCs). During the process, the propeller configuration of tetrakis(4-aminophenyl) ethene molecular with steric hindrance can effectively

suppress the intense π-π stacking interactions of perylene to reduce or even eliminate ACQ. As a result, the ETTA@Pe MCs exhibited a remarkably improved ECL response compared to that of perylene microcrystals alone (Pe MCs).

As a neurotransmitter secreted by the brain, dopamine (DA) has participated in many physiological processes in the body [19]. Scientific studies have indicated that low or absent levels of DA in the brain and central nervous system (CNS) are the main causes of neurological diseases containing depression, schizophrenia and Parkinson's disease [20]. Meanwhile, it represents the activity of effector cells to affect blood pressure, myocardial contraction, blood supply of the kidneys and urine production for playing an important role in the immune, cardiovascular and urinary system [21-23]. Therefore, the determination of DA is of significant importance in clinical disease diagnosis. Herein, shown schematically in Scheme 1, the ECL emission of ETTA@Pe MCs/$S_2O_8^{2-}$ system could be prominently quenched by DA through electron transfer, affording a sensitive quantitative method in biosensor applications. Significantly, the synthesis of ETTA@Pe MCs will expand a new avenue for the settling ACQ of organic luminophores and the rational design of accessible PAHs emitters.

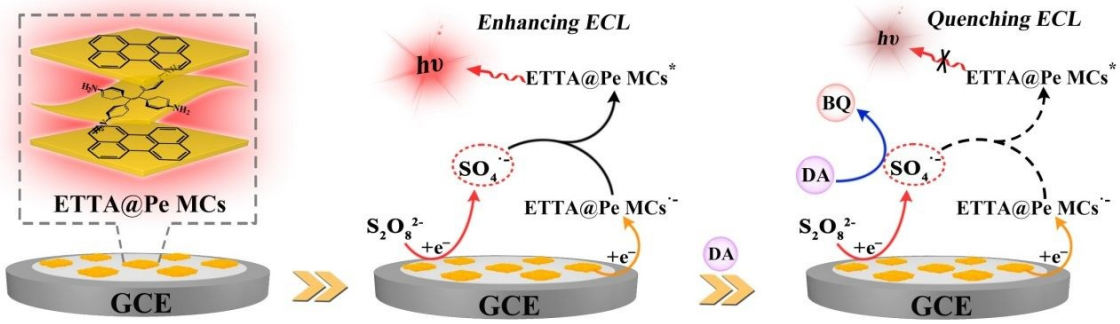

Scheme 1. Sensing platform for DA detection on the basis of ETTA@Pe MCs/$S_2O_8^{2-}$ ECL system, in which BQ represents the oxidation product of DA (dopaquinone).

2. Experiment section

2.1 Reagents and Material.

Perylene was brought from Tokyo Chemical Industry Co. Ltd. (Tokyo, Japan). Tetrakis (4-aminophenyl) ethane (ETTA) was provided by Huawei Ruike Chemical Co. Ltd. (Beijing, China).

Potassium peroxydisulfate, cetyltrimethylammonium bromide (CTAB), tetrahydrofuran (THF), ascorbic acid (AA) and L-histidine (L-His) were supplied from Kelong Chemical Inc. (Chengdu, China). Dopamine (DA) was obtained from bide pharmaceutical technology Co. Ltd. (Shanghai, China). L-cysteine (L-Cys) was received from Ruji Biotechnology Development Co. Ltd. (Shanghai, China). The phosphate buffer saline (PBS, 0.1 M, pH 7.4) consist of 0.1 M KH_2PO_4, 0.1 M Na_2HPO_4 and 0.1 M KCl. The $S_2O_8^{2-}$ solution (10 mM, pH 7.4) was prepared by dissolving a certain amount of solid $K_2S_2O_8$ in 0.1 M PBS. In addition, the other involved solutions in this work were prepared using ultrapure water, which derived from Milli-Q water purification system with an electric resistance of 18.2 MΩ.

2.2 Apparatus.

The cyclic voltammetric (CV) curves and ECL signal were recorded with a CHI 660C electrochemical workstation (Shanghai CH Instruments, China) and a model MPI-E multifunctional analyzer (Xi'An Remax Electronic Science & Technology Co. Ltd., Xi'An, China), respectively. The traditional three-electrode system used with a modified glassy carbon electrode (GCE, Φ = 4 mm) as working electrode, a platinum wire as auxiliary electrode and Ag/AgCl (saturated KCl) or saturated calomel electrode (SCE) as reference electrode in the testing process. The photophysical characterization of different materials was collected by a RF-5301PC spectrofluorophotometer (Shimadzu, Tokyo, Japan) with an excitation source originating from the 150 W xenon lamp (Ushio Inc., Japan). For the ECL emission spectra of different materials, a CHI 760E combined with a Newton EMCCD spectroscopy detector (Andor Co., Tokyo, Japan) was utilized to obtain the 3D ECL spectrum. A scanning electron microscope (SEM, S-4800, Hitachi, Tokyo, Japan) was employed to characterize the surface appearance of ETTA@Pe MCs.

2.3 Synthesis of the Composite Microcrystals (ETTA@Pe MCs).

Tetra-(4-aminobenzene) ethylene-doped perylene composite microcrystals (ETTA@Pe MCs) were prepared based on a reprecipitation method [24]. Firstly, 3 mg Pe powder and 3 mg ETTA powder were simultaneously dissolved in 1 mL of THF organic solvent, sonicating for 10 minutes in an ultrasonic bath.

Subsequently, the ETTA@Pe MCs were synthetized by dropwise addition of the resultant yellow-green solution into 10 mL of CTAB solution (10 mM) under vigorous stirring at a constant temperature of 25 °C for 20 min. Then the product was collected and purified by centrifugation and washing 5 times with ultrapure water, respectively. In the end, the above collected light green product was dispersed into 4 mL of ultrapure water and placed at 4 °C.

2.4 Fabrication of the ECL Biosensor.

As demonstrated in Scheme 1, the bare GCE (4 mm in diameter) first was polished to a mirror surface utilizing 0.3 and 0.05 μm alumina slurry, following by sonication in ultrapure water and ethanol solution, alternately. Then, the ETTA@Pe MCs modified GCE (ETTA@Pe MCs/GCE) was obtained by casting 8 μL of ETTA@Pe MCs on the pretreated GCE surface and was dried naturally at room temperature in the dark.

2.5 Analytical Procedure.

For the quantitative detection of DA, the modified electrode (ETTA@Pe MCs/GCE) was tested with an MPI-A ECL analyzer in 2 mL of $S_2O_8^{2-}$ solution (10 mM, pH 7.4) containing different concentrations of DA. The working potential was set from 0 to -2 V at a scan rate of 0.3 V/s (magnitude 2, PMT high-voltage 700 V).

3. Results and discussion

3.1 SEM Characterization of the ETTA@Pe MCs.

The morphology and size of the prepared ETTA@Pe MCs was characterized by means of SEM technique. According to Fig. 1A, the ETTA@Pe MCs displayed short, block structures with mostly 0.85 μm in wide and 1.30 μm in length. Furthermore, a locally magnified SEM image was clearly exhibited in Fig. 1B. It could be observed that ETTA@Pe MCs possessed a certain thickness and smooth surface.

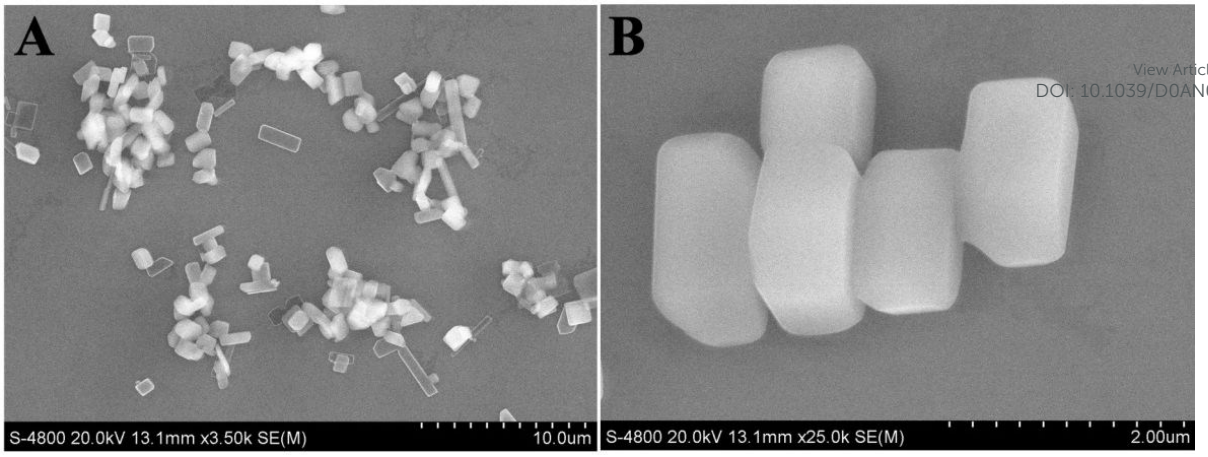

Fig. 1 The SEM image of the ETTA@Pe MCs (A). (B) Partially enlarged picture of (A).

3.2 Luminescence Performances of ETTA@Pe MCs.

The luminescence performances of different nanomaterials were investigated by the combination of 3D ECL and fluorescence (PL) spectral detector. Fig. 2 A and B showed the 3D ECL spectra of ETTA@Pe MCs and Pe MCs, respectively, which were scanned in 0.1 M PBS (pH 7.4) under the potential range of 0 V ~ -2 V. It is worth noting that the ECL intensity of ETTA@Pe MCs (Fig. 2A) was far higher than that of Pe MCs (Fig. 2B). Furthermore, the ECL-potential curve was presented at Fig. 2C to observe the ECL maximum wavelength of two microcrystals intuitively. It can be found the ETTA@Pe MCs exhibited almost 10 times stronger ECL response (curve a) than that of Pe MCs (curve b). Meanwhile, the ECL maximum emission wavelength of ETTA@Pe MCs was located at 582 nm (curve a), comparing with that of Pe MCs at 604 nm (curve b). The blue shift can be inferred the intense π-π stacking interactions of the perylene monomers in the ETTA@Pe MCs was inhibited effectively by doping the non-planar molecular ETTA. Furthermore, PL spectra of ETTA@Pe MCs and Pe MCs were also investigated to confirm the above speculation. At an excitation wavelength of 372 nm, pure Pe MCs displayed the maximum emission peak wavelength at 555 nm (Fig. 2D, curve b). While the maximum emission peak of the ETTA@Pe MCs blue shifted to 488 nm (Fig. 2D curve a). The experimental results provided the evidence that the doping of ETTA molecule in Pe microcrystals could decrease the aggregation of Pe to eliminate the ACQ and achieve the significantly enhanced the electro/photo-generated emission of Pe in aggregates.

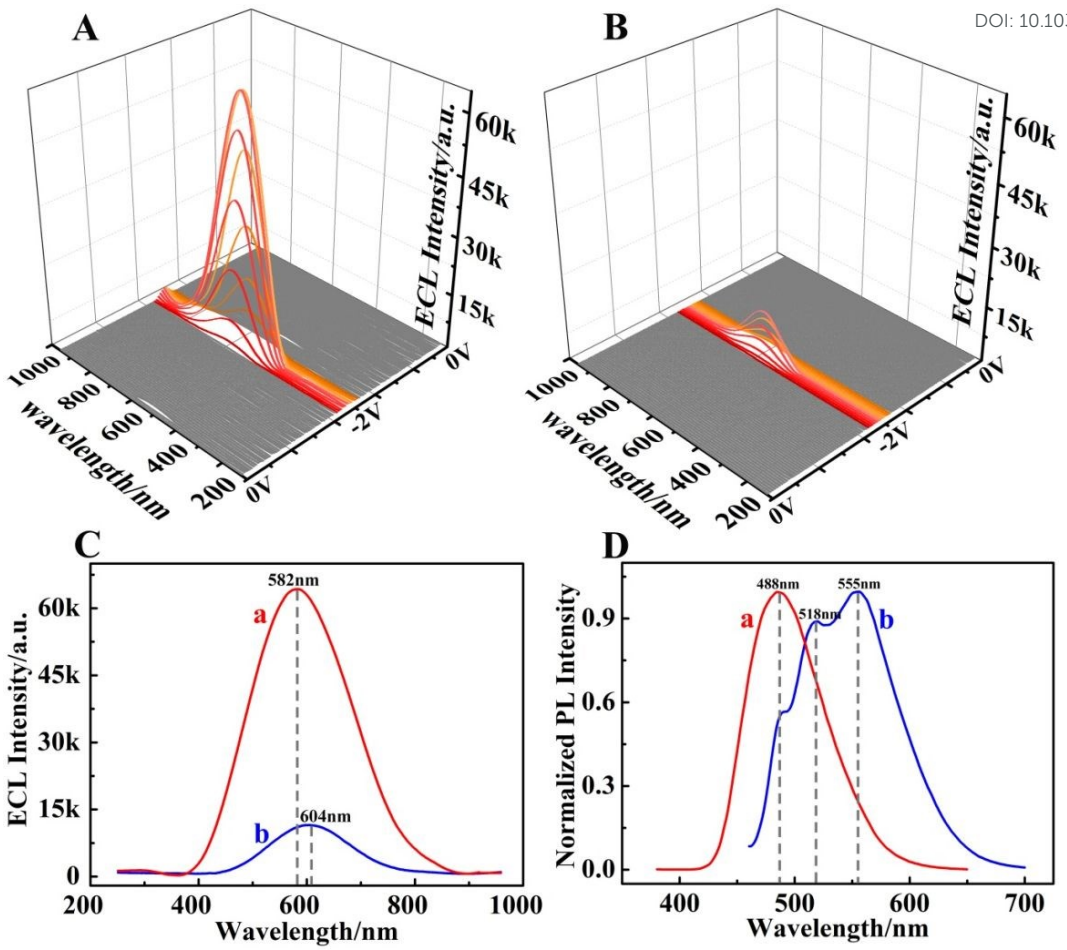

Fig. 2 3D ECL spectra of the ETTA@Pe MCs (A) and the Pe MCs (B). (C) 2D ECL spectra of the ETTA@Pe MCs (curve a) and Pe MCs (curve b). (D) Normalized PL emission spectrum of the ETTA@Pe MCs (curve a, λex=372 nm) and Pe MCs (curve b, λex=372 nm).

3.3 The Possible ECL-Enhancing Mechanism.

The ECL-potential responses were performed to demonstrate the ECL reaction mechanism of ETTA@Pe MCs. As presented in Fig. 3A, the bare GCE (curve a) and ETTA MCs modified GCE (ETTA MCs/GCE, curve b) showed no distinct ECL emission in PBS due to the lack of ECL luminophores. It is worth noting that feeble ECL responses could be seen when Pe MCs and ETTA@Pe MCs modified GCE (curve c, Pe MCs/GCE and curve d, ETTA@Pe MCs/GCE) were detected in PBS. The reason why the ECL responses were feeble was that the coreactant was the inactive dissolved O_2. Subsequently, the $S_2O_8^{2-}$ as a kind of active coreactant was added in PBS. As shown in Fig. 3B, there still no distinct ECL responses at bare GCE (curve a) and ETTA MCs/GCE (curve b). As expected, Pe MCs/GCE exhibited an

obvious ECL emission with the peak intensity about 1675 a.u. (curve c), while the ECL response of ETTA@Pe MCs/GCE was dramatically enhanced to 16813 a.u. (curve d), which was almost 10 times stronger than that of Pe MCs/GCE. The results indicated the propeller configuration of ETTA with steric hindrance could restrain the intermolecular π-π stacking interactions of perylene effectively to reduce or even eliminate ACQ for effectively improving the ECL performance of Pe MCs.

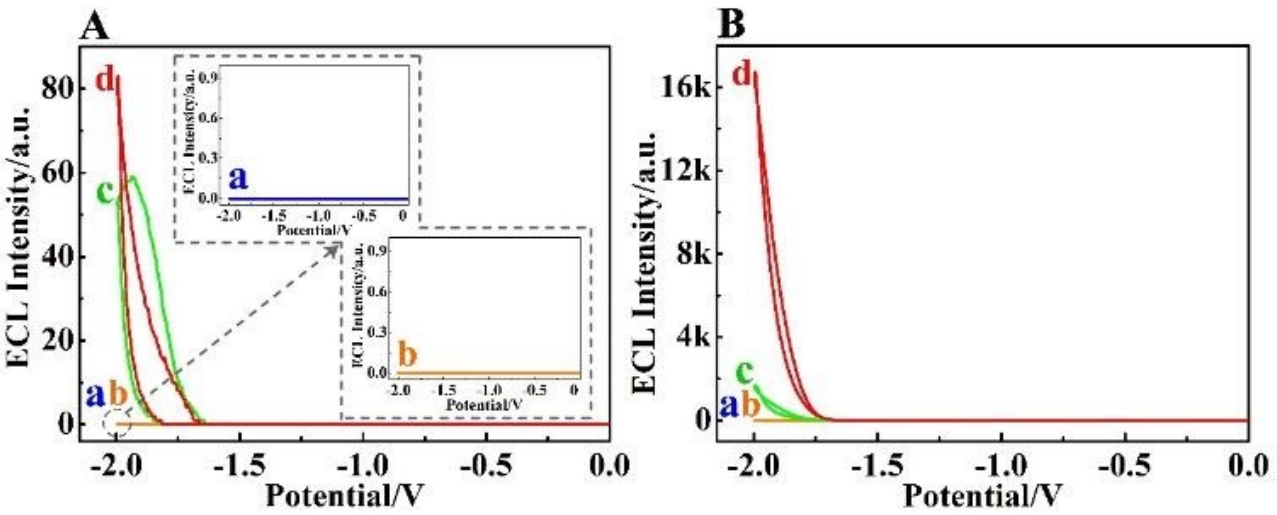

Fig. 3 (A) ECL-potential responses of bare GCE (curve a), ETTA MCs/GCE (curve b), Pe MCs/GCE (curve c) and ETTA@Pe MCs/GCE (curve d) in PBS (pH 7.4). (B) ECL-potential responses of bare GCE (curve a), ETTA MCs/GCE (curve b), Pe MCs/GCE (curve c) and ETTA@Pe MCs/GCE (curve d) in PBS (pH 7.4) containing 10 mmol/L $S_2O_8^{2-}$.

3.4 ECL Responses of the Biosensor toward DA.

Under the optimum experimental conditions, the performance of ETTA@Pe MCs/GCE biosensor for DA detection was assessed in 10 mmol/L $S_2O_8^{2-}$ solution (pH 7.4) containing DA with different concentrations. As showed in Fig. 4A, the ECL signal decreased accordingly as the concentration of DA elevated from 1 nmol/L to 100 μmol/L (curve *a* to *h*). And a good linear relationship between the changes in ECL intensities (ΔI_{ECL}) and the logarithmic value of DA concentrations was presented in Fig. 4B. The linear equation was fitted as $\Delta I = 8097.9 - 2426.9\lg c_{DA}$ with a squared correlation coefficient (R^2) of 0.9969. Moreover, a detection limit of 0.96 nmol/L for the test platform could be calculated based on 3σ rule [25]. Significantly, the comparison results among diverse methods for DA detection were listed in Tab. 1.

View Article Online
DOI: 10.1039/D0AN00997K

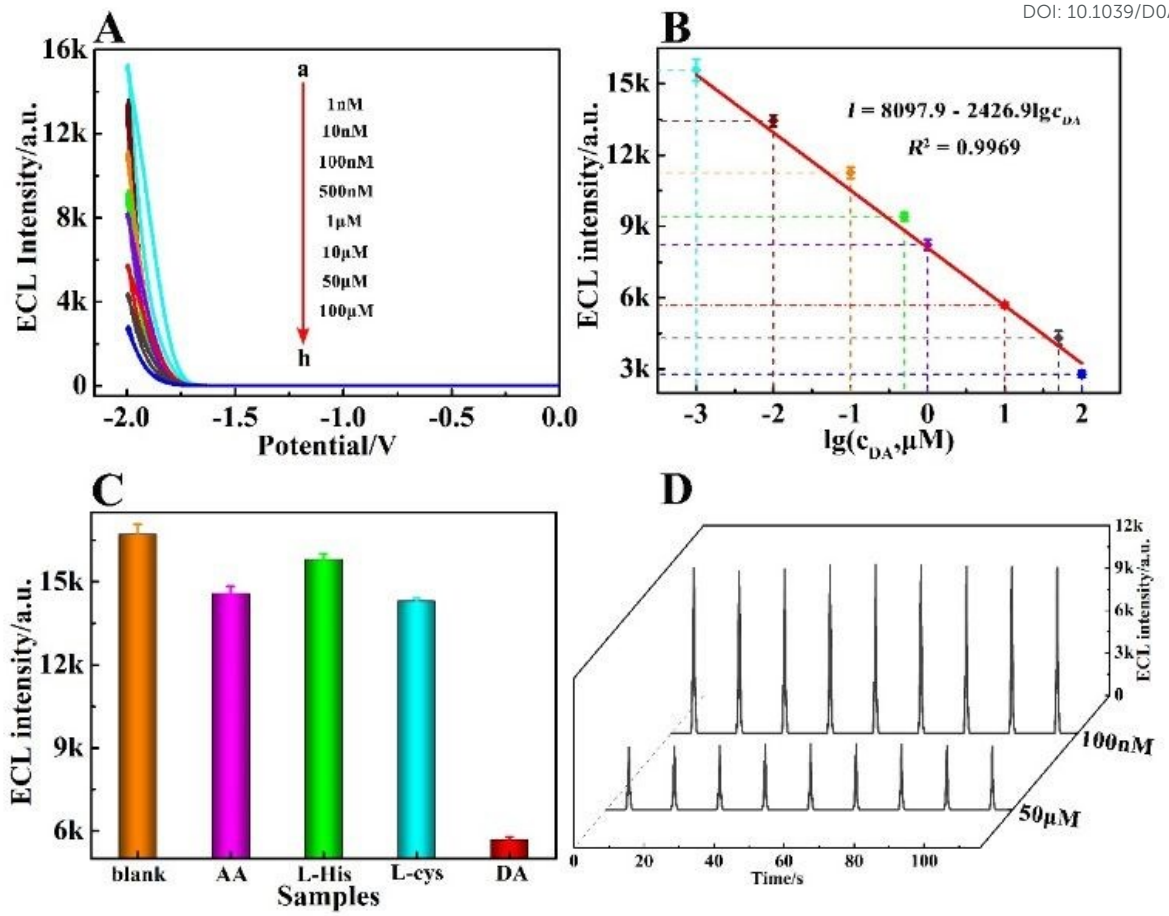

Fig. 4 (A) ECL responses of the proposed biosensor upon addition of different concentrations for DA in 10 mmol/L $S_2O_8^{2-}$ solution (pH 7.4). The concentrations of DA as follow: 1.0 nmol/L, 10 nmol/L, 100 nmol/L, 500 nmol/L, 1.0 μmol/L, 10 μmol/L, 50 μmol/L, 100 μmol/L (from a to h). (B) Calibration plot for DA determination. (C) Selectivity of the developed biosensor over various interference: AA, L-His and L-Cys (100 μmol/L). (D) Stability assessment of the biosensor for 50 μmol/L and 100 nmol/L DA.

Tab. 1 The comparison results among diverse methods for DA detection.

Method	Linear range	LOD	Ref
PL	10 nM - 10 mM	4.8 nM	[26]
Electrochemistry	2 nM - 600 nM	0.4 nM	[27]
Chemiluminescence	5.6 nM - 55.6 μM	1.87 nM	[28]
Colorimetric method	2 μM - 55 μM	0.76 μM	[29]
ECL	500 nM - 1 mM	0.35 μM	[30]
ECL	1 nM -100 μM	0.96 nM	The work

3.5 Selectivity and Stability of the Biosensor.

The specificity of the ECL biosensor for DA was evaluated in the presence of the possible interfering substances (AA, L-His and L-Cys) at a concentration of 100 μmol/L. As showed in Fig. 4C, the ECL intensities of biosensor with above interfering substances demonstrated only a slight decrease compared to that of the blank solution. However, the ECL signal of the proposed biosensor declined significantly in the presence of DA at 10 μmol/L. These results indicated that the satisfactory selectivity of proposed method for DA determination. In addition, the stability investigation was executed via consecutive ECL scanning for 9 cycles using 50 μmol/L and 100 nmol/L of DA as models, respectively. According to Fig. 4D, the ECL responses simultaneously exhibited no obvious fluctuation, manifesting the developed biosensor had good stability.

4. Conclusions

In the work, the ECL performance of perylene microcrystals was promoted dramatically by doping the propeller configuration of ETTA with steric hindrance to effectively suppress the ACQ effect for the first time. As a result, the ETTA@Pe MCs exhibited almost 10 times stronger ECL signal compared to that of Pe MCs, which provided a facile platform for ultrasensitive detection of DA with limit of detection down to 0.96 nmol/L. This work proposed a facile and economic method for the inhibition of the negative π–π stacking to make use of the planar polycyclic aromatic hydrocarbons (PAHs) with ACQ in biosensing.

Declaration of interests

There are no conflicts to declare.

View Article Online
DOI: 10.1039/D0NR03971

Acknowledgements

This work was financially supported by the NNSF of China (21904108 and 21675130), the Natural Science Foundation Project of CQ CSTC (cstc2018jcyjAX0546), and the Fundamental Research Funds for the Central Universities (XDJK2019TJ002), China.

Notes and references

[1] P.M. Beaujuge, J.R. Reynolds, *Chem. Rev.*, 2010, **110**, 268.

[2] J.E. Dick, C. Renault, B.K. Kim and A.J. Bard, *J. Am. Chem. Soc.*, 2014, **136**, 13546.

[3] N. Meher, S. Panda, S. Kumarb, P. K. Iyer, *Chem. Sci.*, 2018, **9,** 3978.

[4] Y.J. Huang, J. Xing, Q.Y. Gong, L.C. Chen, G.F. Liu, C.J. Yao, Z.R. Wang, H.L. Zhang, Z. Chen, Q.C. Zhang, *Nat. Commun.*, 2019, **10**, 169.

[5] J.E. Dick, C. Renault, B.K. Kim, A.J. Bard, *J. Am. Chem. Soc.*, 2014, **136**, 13546.

[6] Z.G. Han, Z.F. Yang, H.S. Sun, Y.L. Xu, X.F. Ma, D.L. Shan, J. Chen, S.H. Huo, Z. Zhang, P.Y. Du, and X.Q. Lu, *Angew. Chem. Int. Ed.,* 2019, **58,** 5915.

[7] Y.N. Hong, J. W.Y. Lam, B.Z. Tang, *Chem. Soc. Rev.*, 2011, **40**, 5361.

[8] L.Y. Zong, H.Q. Zhang, Y.Q. Li, Y.B. Gong, D.Y. Li, J.Q. Wang, Z. Wang, Y.J. Xie, M.M. Han, Q. Peng, X.F. Li, J.F. Dong, J. Qian, Q.Q. Li, Z. Li, *ACS Nano.,* 2018, **12**, 9532.

[9] J.M. Delente, D. Umadevi, S. Shanmugaraju, O. Kotova, G.W. Watson, T. Gunnlaugsson, *Chem. Commun.*, 2020, **56**, 2562-2565.

[10] Z. Zhao, S.M. Gao, X.Y. Zheng, P.F. Zhang, W.T. Wu, R.T. K. Kwok, Y. Xiong, N. L. C. Leung, Y. Chen, X. Gao, J.W.Y. Lam, B.Z. Tang, *Adv. Funct. Mater.*, 2018, **28**, 1705609.

[11] X.J. Zheng, W.C. Zhu, C. Zhang, Y. Zhang, C. Zhong, H. Li, G.H. Xie, X.J. Wang, C.L. Yang, *J. Am. Chem. Soc.*, 2019, **141,** 4704.

[12] M.H. Xie, W. Cai, X. Chen, R.F. Guan, L.M. Wang, G.H. Hou, X.G. Xi, Q.F. Zhang, X.L. Yang, R. Shao, *ACS Appl. Mater. Interfaces*, 2018, **10**, 2868.

[13] J. Yu, Y. Cui, H. Xu, Y. Yang, Z. Wang, B. Chen and G. Qian, *Nat. Commun.*, 2013, **4**, 2719.

[14] H.Y. Chih, Y.W. Chen, Y.C. Hsieh, W.C. Li, C.W. Liao, C.H. Lin, T.Y. Chiu, W.W. Tsai, C.W. Lu, C.H. Chang, *Chem. Eur. J.*, 2019, **25**, 16699.

[15] J.D. Luo, Z.L. Xie, J.W. Y. Lam, L. Cheng, H.Y. Chen, C.F. Qiu, H.S. Kwok, X.W. Zhan, Y.Q. Liu, D.B. Zhu, B.Z. Tang, *Chem. Commun.*, 2001, **19**, 1740.

[16] Q.L. Zhao, S. Zhang, Y. Liu, J. Mei, S.J. Chen, P. Lu, A.J. Qin, Y.G. Ma, J.Z. Sun, B.Z. Tang, *J. Mater. Chem.* 2012, **22**, 7387.

[17] Q.L. Zhao, X.A. Zhang, Q. Wei, J. Wang, X.Y. Shen, A.J. Qin, J.Z. Sun, B.Z. Tang, *Chem. Commun.*, 2012, **48**, 11671.

[18] L.Y. Zong, H.Q. Zhang, Y.Q. Li, Y.B. Gong, D.Y. Li, J.Q. Wang, Z. Wang, Y.J. Xie, M.M. Han, Q. Peng, X.F. Li, J.F. Dong, J. Qian, Q.Q. Li, Z. Li, *ACS Nano*, 2018, **12**, 9532.

[19] J. Li, H.F. Shen, S.H. Yu, G.S. Zhang, C.L. Ren, X.Y. Hu, Z.J. Yang, Analyst, 2020, **145**, 3283.

[20] N. Maouche, N. Ktari, I. Bakas, N. Fourati, C. Zerrouki, M. Seydou, F. Maurel, M. M. Chehimi, *J. Mol. Recognit.*, 2015, **28**, 667.

[21] S. Basu, P. S. J. Dasgupta, *J. Neuroimmunol.*, 2000, **102**, 113.

[22] S.J. Zhuo, Y.Y. Guan, H. Li, J. Fang, P. Zhang, J.Y. Du, C.Q. Zhu, *Analyst*, 2019, **144**, 656.

[23] M.F. Lokhandwala, F. Amenta, *FASEB J.*, 1991, **5**, 3023.

[24] W.R. Cai, G.Y. Zhang, K.K. Lu, H.B. Zeng, S. Cosnier, X.J. Zhang, D. Shan, *ACS Appl. Mater. Interfaces*, 2017, **9**, 20904.

[25] C.K. Dixit, S.K. Vashist, F.T. O'Neill, B. O'Reilly, B.D. MacCraith, R. O'Kennedy, *Anal. Chem.*, 2010, **82**, 7049.

[26] Y.X. Lan, F. Yuan, T.H. Fereja, Wang, C. Wang, B.H. Lou, J.P. Li, G.B. Xu, *Anal. Chem*. 2019, **91**, 2135-2139.

[27] Q.L. Yuan, Y. Liu, C. Ye, H.Y. Sun, D. Dai, Q.P. Wei, G.S. Lai, T.Z. Wu, A.M. Yu, L. Fu, K.W.A. Chee, C. T. Lin, *Biosens. Bioelectronic.*, 2018, **111**, 117.

[28] Y.X. Lan, F. Yuan, T.H. Fereja, C. Wang, B.H. Lou, J.P. Li, G. B. Xu, *Anal. Chem.* 2019, **91**, 2135.

[29] M.N. Ivanova, E.D. Grayfer, E.E. Plotnikova, L.S. Kibis, G. Darabdhara, P.K. Boruah, M.R. Das, V.E. Fedorov, *ACS Appl. Mater. Interfaces*, 2019, **11**, 22102.

[30] F. Wang, J. Lin, H.Y. Wang, S.S. Yu, X.Q. Cui, A. Ali, T. Wu, Y. Liu, *Nanoscale*, 2018, **10**, 15932.